Smart Full-Exploitation of Beamforming Fusion assisted Spectrum Sensing for Cognitive Radio

Sarra Ben Chaabane
Laboratory Sys'Com-ENIT (LR-99-ES21)
Tunis El Manar University
Tunis, Tunisia
sarra.benchaabane@enit.utm.tn

Kais Bouallegue
Univ Rennes, INSA Rennes
CNRS, IETR - UMR 6164
Rennes, France
kais.bouallegue@insa-rennes.fr

Akram Belazi
Laboratory RISC-ENIT (LR-16-ES07)
Tunis El Manar University
Tunis, Tunisia
akram.belazi@enit.utm.tn

Sofiane Kharbech
Laboratory Sys'Com-ENIT (LR-99-ES21)
Tunis El Manar University
Tunis, Tunisia
sofiane.kharbech@ieee.org

Ammar Bouallegue
Laboratory Sys'Com-ENIT (LR-99-ES21)
Tunis El Manar University
Tunis, Tunisia
ammarbouallegue.syscom@gmail.com

***Abstract*—This paper proposes blind spectrum sensing (SS) in a narrowband context called Beamforming Fusion assisted Spectrum Sensing (BFSS). Considering a channel with angles of arrival (AoA), we jointly exploit beamforming algorithms to make decisions about the detection of users on frequency resources. The proposed method is totally blind and does not require knowledge of the noise power, the channel estimation, and the source signal. A state-of-the-art comparison of SS methods using beamforming is provided to validate our contribution in a shallow SNR region.**

***Index Terms*—Cognitive radio, spectrum sensing, fusion detection, beamforming.**

I. Introduction

Mobile communication operates in a heterogeneous environment and needs to be supported by flexible spectrum management capabilities. Cognitive radio (CR) is a promising technology that can overcome the various problems due to static spectrum allocation. Indeed, the CR system can adapt to its electromagnetic environment. By modifying its radio configuration, the CR system can opportunistically use any free spectral resource [1].

Furthermore, the next generation of mobile radio networks and the increased development of connected technologies, such as the Internet of things (IoT) [2] and vehicle to everything communication (V2X) [3], will lead to a scarcity of the frequency resources. Therefore, it is essential to find solutions to meet the needs of these different communication technologies.

In CR networks, we define two main kinds of users. On the one hand, we describe the first user called the primary user (PU), who has all the priorities on the spectral resource. And in the other hand, the second user is called the secondary user (SU). SU is considered the CR system, which opportunistically exploits the unused frequency resource.

The main idea of the SU is to exploit the best resource opportunity to reallocate unused frequency bands dynamically. Thus, the SU must in no way interfere with the PU communication. So the SU has to be aware of its electromagnetic environment to avoid dismissing resource opportunities and not interfere with the PU. The CR system is based on the cognition loop built on the spectrum sensing (SS) [4].

Some SS methods consider that the SU has *a priori* knowledge of the noise power, the source signal, or the channel, such as matched-filter, energy detection (ED), and cyclostationarity detector. Recent blind SS algorithms exploit the multiple-input multiple-output (MIMO), in order to improve the detection of the PU: blindly combined energy detection (BCED) [5], arithmetic-to-geometric mean (AGM) [6], maximum-eigenvalue-geometric-mean (MEGM) [7] and mean-to-square extreme eigenvalue (MSEE) [8]. To improve the PU detection [9], recent contributions proposed beamforming such as maximum energy beamforming-output-to-input (MEBOI) [10], maximum-to-minimum beam energy (MMBE) [11] and maximum-to-mean energy detector (MMED) [12]. In [13], the authors propose a beamformer-aided support vector machine model to improve the PU detection. More recent SS methods based on the machine learning approaches have been proposed [14] [15].

In this paper, we propose to investigate the performance of the full exploitation of several beamforming algorithms. This new SS approach based on beamforming takes advantage of all the SS algorithms based on beamforming to make decisions on the presence of the PU. Therefore, the idea is to exploit the processing carried out at the receiver by beamforming and maximize decision-making reliability. Finally, simulation results show that our design performs better than the classical beamforming algorithms in the literature for different scenarios.

The rest of the paper is organized as follows. Section II introduces the system model. Section III provides the background work, including some SS methods based on the beamforming method. In section IV, we provide our contribution and the algorithm. In section V, simulation results evaluate the performance of the proposed method, and the conclusion

978-1-6654-6975-3/22/$31.00 ©2022 IEEE

is finally summarized in section VI.
Boldface lower letter is used to denote vectors and boldface capital letter to denote matrices. We use superscript $(.)^T$, $(.)^*$ and $(.)^H$ to denote transpose, complex conjugate, and Hermitian (complex conjugate transpose), respectively. $\mathbf{I}_q$ denotes the identity matrix of order q and $E[.]$ stands for expectation operation.

II. System Model

Here, we consider a static flat fading channel described in [16]. The SU is a CR terminal with multiple uniform linear antennas (ULA). In the SS paradigm, two main hypotheses are defined, on the one hand, there is $\mathcal{H}_0$ when the frequency resource is free, and, on the other hand, $\mathcal{H}_1$, when the PU is present. Thus, we can note the following probabilities

- Detection (Power of test) as $P_d = \mathrm{P}(\mathcal{H}_1;\mathcal{H}_1)$
- False alarm (Type I error) as $P_{fa} = \mathrm{P}(\mathcal{H}_1;\mathcal{H}_0)$.
- Miss-detection (Type II error) as $P_{md} = \mathrm{P}(\mathcal{H}_0;\mathcal{H}_1)$

where $P(\mathcal{H}_\varepsilon;\mathcal{H}_\varsigma)$ indicates the probability of deciding $\mathcal{H}_\varepsilon$ when $\mathcal{H}_\varsigma$ is true [17].

The received signal by the SU at the uniform linear array (ULA) antenna configuration is expressed as

$$\mathcal{H}_0 \quad : \quad x_m(n) = b_m(n) \tag{1}$$
$$\mathcal{H}_1 \quad : \quad x_m(n) = r_m(n) + b_m(n), \tag{2}$$

where m describes the m^{th} antenna $(m = 0, \cdots, (M-1))$, $x_m(n)$ is the received signal at the antenna m, $r_m(n)$ is the PU's signal received by SU through the channel propagation and $b_m(n)$ is a zero-mean additive white Gaussian noise with variance σ_b^2. The PU's signal is received by the SU via AoA noted ψ. Therefore, we note the n^{th} received sample at the antenna m is expressed as

$$x_m(n) = \varpi \sum_{p=0}^{P-1} \sum_{\psi_p \in A} a_{mp}(\psi_p) s_p(n - i(\psi_p)) + b_m(n), \tag{3}$$

where P is the number of PU, A is the set of paths including all AoA, $\varpi = \{0, 1\}$ under $\mathcal{H}_\varpi$ hypothesis, ψ_p is the AoA of the p^{th} PU's signal, $s_p(n)$ represents the source signal from p^{th} PU to the CR receiver antennas, $i(.)$ represents the delay and $a_{mp}(\psi_p)$ is the gain path between the p^{th} PU and the m^{th} antenna. We consider a ray propagation channel modeled by the steering vector as defined in [18]. So, the gain path $a_{mp}(\psi_p)$ between the p^{th} PU and the m^{th} antenna of the SU is given by

$$a_{mp}(\psi_p) = a_{0p}(\psi_p) \exp\left(2j\pi m\alpha(\psi_p)\right), \tag{4}$$

where $a_{0p}(\psi_p)$ is the path gain between the SU and the first antenna $\alpha(\psi_p) = \frac{d}{\lambda} cos(\psi_p)$, λ is the wavelength and d is the distance between two consecutive antennas. In [19], the best trade-off between the cancellation of sidelobe effect and the coupling of the ULA antenna is investigated and the result is obtained for $d = \lambda/2$. From (3) and (4), we can note

$$x_m(n) = \sum_{p=0}^{P-1} \sum_{\psi_p \in A} a_{0p}(\psi_p) \exp\left(2j\pi m\alpha(\psi_p)\right) \times s_p(n - i(\psi_p)) + b_m(n). \tag{5}$$

Under the multipath channel context, as depicted in Fig. 1, each path includes a gain path and AoA. The received signal by the SU can be expressed as

$$\sum_{\psi_p \in A} a_{mp}(\psi_p) s_p(n - i(\psi_p)) = \sum_{i=0}^{C_p} \sum_{\psi_p \in A_i} s_p(n-i) a_{mp}(\psi_p), \tag{6}$$

where $\psi_p \in A_i$ is denoted for all the AoA of A having the same delay i and C_p is the channel order. Thus, the received signal at the m^{th} antenna of the SU can be finally expressed as

$$x_m(n) = \sum_{p=0}^{P-1} \sum_{i=0}^{C_p} h_{mp}(i) s_p(n-i) + b_m(n), \tag{7}$$

where $h_{mp}(i) = \sum_{\psi_p \in A_i} a_{mp}(\psi_p)$. For the sequel, we define the following vectors.

$$\boldsymbol{x}^T(n) = [x_0(n), x_1(n), \cdots, x_{M-1}(n)], \tag{8}$$
$$\boldsymbol{b}^T(n) = [b_0(n), b_1(n), \cdots, b_{M-1}(n)] \tag{9}$$
$$\boldsymbol{s}_p^T(n) = [s_p(n), s_p(n-1), \cdots, s_p(n - C_p + 1), \tag{10}$$

where $\boldsymbol{x}^T(n)$ is the received signal vector, $\boldsymbol{b}^T(n)$ is the noise vector and $\boldsymbol{s}_p^T(n)$ is the source signal. The received signal at the SU from the PU under $\mathcal{H}_1$ hypothesis is expressed as $\boldsymbol{x}(n) = \boldsymbol{H}\boldsymbol{s}(n) + \boldsymbol{b}(n)$, where $\boldsymbol{H}$ is a $M \times (C+P)$ matrix which represents the channel, $\boldsymbol{H} = [\boldsymbol{H}_0, \boldsymbol{H}_1, \cdots, \boldsymbol{H}_{P-1}]$ where $\boldsymbol{H}_p$ is a $M \times (C_p)$ channel matrix between p^{th} PU and the receiver as described in [8] and $C = \sum_{p=0}^{P-1} C_p$.

III. Background work

Here, we first introduce the standard beamforming process realized at the receiver's antennas. Then, the beamforming approach in this article is depicted, and some SS algorithms exploiting this spatial filter combined with energy are introduced. All of the SS algorithms described in this paper are totally blind, which means that the SU has no a priori knowledge of the PU's signal, the noise power, or the channel state information.

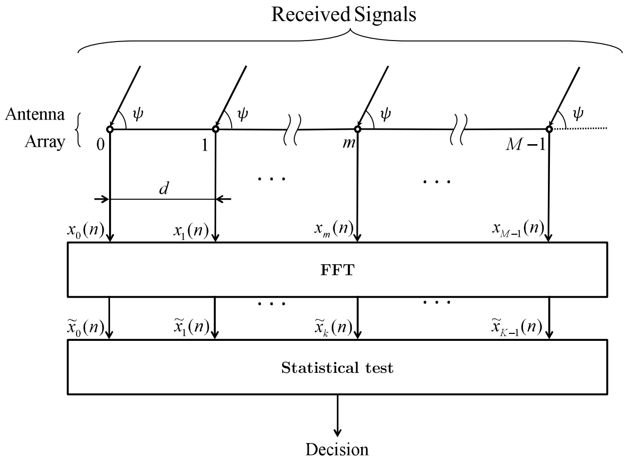

Fig. 1: Schematic of the energy-based spectrum detector and spatial filtering under a single incident angle.

A. Conventional Beamformer

Considering k directionally-weighted outputs vector system expressed as $\boldsymbol{w}_k = [w_{0k}, w_{1k}, \cdots, w_{(M-1)k}]^T$, the received signal is expressed as

$$\tilde{x}_k(n) = \boldsymbol{w}_k^H \boldsymbol{x}(n) = \boldsymbol{w}_k^H \boldsymbol{u}(n) + \boldsymbol{w}_k^H \boldsymbol{b}(n), \quad (11)$$

$$\tilde{\boldsymbol{x}}(n) = \boldsymbol{W}^H \boldsymbol{x}(n) = \boldsymbol{W}^H \boldsymbol{u}(n) + \boldsymbol{W}^H \boldsymbol{b}(n), \quad (12)$$

where $\tilde{\boldsymbol{x}}(n) = [\tilde{x}_0(n), \tilde{x}_1(n), \cdots, \tilde{x}_{M-1}(n)]^T$ is the post processing received signal, $\boldsymbol{W} = [\boldsymbol{w}_0, \boldsymbol{w}_1, \cdots, \boldsymbol{w}_{M-1}]$ is the weighted matrix and $\boldsymbol{u}(n) = [u_0(n), u_1(n), \cdots, u_{M-1}(n)]^T$ is the source signal. To reduce the computational complexity of the beamforming process for the CR, we choose the Fourier transform (FT) as the the directionally-weighted vector. Indeed, by considering $w_{mk} = \exp\left(-2j\pi m \frac{k}{M}\right)$, the spatial filter becomes the fast FT (FFT) processing with K outputs [20]

As depicted in Fig. 1, the statistical test is evaluated and finally compared to the pre-computed fixed threshold to decide between $\mathcal{H}_0$ and $\mathcal{H}_1$ hypothesis.

We respectively express the covariance matrix of the input and the output of the FFT as

$$\mathbf{R}_x(N) = \frac{1}{N} \sum_{n=1}^{N} \mathbf{x}(n)\mathbf{x}(n)^H, \quad (13)$$

$$\mathbf{R}_{\tilde{x}}(N) = \frac{1}{N} \sum_{n=1}^{N} \tilde{\mathbf{x}}(n)\tilde{\mathbf{x}}(n)^H, \quad (14)$$

where N is the number of samples corresponding to the detection time, in totally blind SS methods, the threshold is computed using the analytical expression of the P_{fa}.

B. Maximum Energy Beamforming-Output-to-Input (MEBOI)

In [16], the authors introduced the MEBOI algorithm based on comparing the maximum distributed energy in the input and the output of the spatial filter process. In the $\mathcal{H}_1$ hypothesis, the energy at the inputs of the beamforming process is uniformly distributed whereas, at the output process, the energy will be concentrated on only one output corresponding to the AoA. Thus, to exploit the input and output energy distribution, the statistical test of the MEBOI algorithm is based on the ratio of the maximum energy evaluated from the beamforming process and the maximum energy before the spatial filter.

The statistical test of the MEBOI algorithm is expressed as

$$T_{MEBOI} = \frac{E_O}{E_I} \underset{\mathcal{H}_1}{\overset{\mathcal{H}_0}{\lessgtr}} \gamma_{MEBOI}, \quad (15)$$

where $E_O = \max_k \left(\mathbf{R}_{\tilde{x}}(N)\right)_{kk}$, $E_I = \max_m \left(\mathbf{R}_x(N)\right)_{mm}$ and γ_{MEBOI} is the threshold analytically expressed in [10] of the MEBOI detector.

C. Maximum-to-Minimum Beam Energy (MMBE)

On the other hand, the MMBE algorithm considers only the outputs of the beamforming process. This totally blind detection method provides good results compared to the classical SS algorithms. Thus, under the $\mathcal{H}_1$ hypothesis, by exploiting the gap of the outputs energy of the spatial filter, the MMBE method evaluates the maximum and minimum energy ratio. The statistical test is defined as

$$T_{MMBE} = \frac{E_M}{E_m} \underset{\mathcal{H}_1}{\overset{\mathcal{H}_0}{\lessgtr}} \gamma_{MMBE}, \quad (16)$$

where $E_m = \underset{k}{min} \left(\mathbf{R}_{\tilde{x}}(N)\right)_{kk}$, $E_M = \underset{k}{max} \left(\mathbf{R}_{\tilde{x}}(N)\right)_{kk}$ and γ_{MMBE} is the threshold of the MMBE algorithm expressed in [20].

D. Maximum-to-Mean Energy Detector (MMED)

MMED detector is also based on the output of the spatial filter. This method is based on the ratio of the maximum energy to the mean one of the output of the beamformer. The statistical test is expressed as

$$T_{MMED} = \frac{E_M}{\mathcal{M}} \underset{\mathcal{H}_1}{\overset{\mathcal{H}_0}{\lessgtr}} \gamma_{MMED}, \quad (17)$$

where $\mathcal{M} = \frac{1}{M} \sum_{k=0}^{M-1} (\boldsymbol{R}_{\tilde{\boldsymbol{x}}}(N))_{kk}$ represents the mean received energy and γ_{MMED} is the threshold analytically proposed in [12] based on the P_{fa}.

IV. Beamforming Fusion assisted Spectrum Sensing (BFSS)

In this section, we introduce our contribution consisting of the unification of all SS algorithms presented in the previous section.

This new algorithm, called Beamforming Fusion assisted Spectrum Sensing (BFSS), optimizes the spatial filtering process. Indeed, knowing that the spatial filtering operation is performed at least once, it is interesting to exploit all evaluated energies from all directions. In this sight, we exploit all the methods based on beamforming at the same time. Knowing that the computation of the statistical test is not heavy, we take advantage of each detector.

Algorithm 1 Algorithm for BFSS detector

Input: N and M.
Output: $\mathcal{D}_{BFSS}$
Initialization:
- The probability of false alarm is fixed at 10%
- Compute the threshold of MEBOI expressed in [10].
- Compute the threshold of MMBE expressed in [20].
- Compute the threshold of MMED expressed in [12].

Compute the covariance matrix of the received signal $\mathbf{R}_x(N) = \dfrac{1}{N}\sum_{n=1}^{N} \mathbf{x}(n)\mathbf{x}(n)^H$. (13)
Compute the covariance matrix of the received signal spatially filtered $\mathbf{R}_{\tilde{x}}(n) = \frac{1}{N}\sum_{n=1}^{N} \tilde{\mathbf{x}}(n)\tilde{\mathbf{x}}(n)^H$. (14)
if $\mathcal{D}_{MEBOI}$ **or** $\mathcal{D}_{MMBE}$ **or** $\mathcal{D}_{MMED}$ **then**
    $\mathcal{D}_{BFSS} \leftarrow$ **true**
else if not $\mathcal{D}_{MEBOI}$ **and not** $\mathcal{D}_{MMBE}$ **and not** $\mathcal{D}_{MMED}$ **then**
    $\mathcal{D}_{BFSS} \leftarrow$ **false**
end if
return $\mathcal{D}_{BFSS}$

During the initialization phase, we calculate, from the number of antennas M and the detection time N, the thresholds of the different detection methods {MEBOI, MMBE, MMED} for a P_{fa} of 0.1. Then, in the second step, we evaluate the covariance matrices presented in (13) and (14). The diagonal entries of these covariance matrices represent the energy of the received signal in (13) and the energy from different sectors in (14). These entries are exploited to compute the statistical tests of the algorithm based on beamforming. The result of the comparison of each statistical test and its threshold is a boolean expression denoted as $\mathcal{D}_j$ ($j =$ {MEBOI, MMBE, MMED}). Finally, if only one $\mathcal{D}_j$ is true, the decision on $\mathcal{D}_{BFSS}$ is true.

In order to understand our contribution, we propose the algorithm of the BFSS approach.

V. Simulations and Discussion

In this section, we evaluate the performance of the proposed spectrum sensing algorithms BFSS. We compare our approach to the other ones based on the beamforming method and the MME [21] algorithm based on the eigenvalue decomposition of the covariance matrix of the received signal using the MATLAB R2020a version.

a) Parameters of the simulation: We consider only one PU. The source signal from the PU is a BPSK modulated signal. Some parameters have the same values throughout simulations unless otherwise indication $P = 1$, $C_p = 0$, $M = 5$, $N = 1000$ and $\psi \in [0, \pi]$ (uniformly distributed).

b) Simulation results for different SNR: In Fig. 2, we compare the proposed method BFSS to the other methods based on the beamforming approach. We can see that the BFSS method outperforms other SS algorithms. Indeed, for an SNR $= -16$ dB, $P_d\{BFSS\} = 0.915$ and $P_d\{MMED\} = 0.82$.

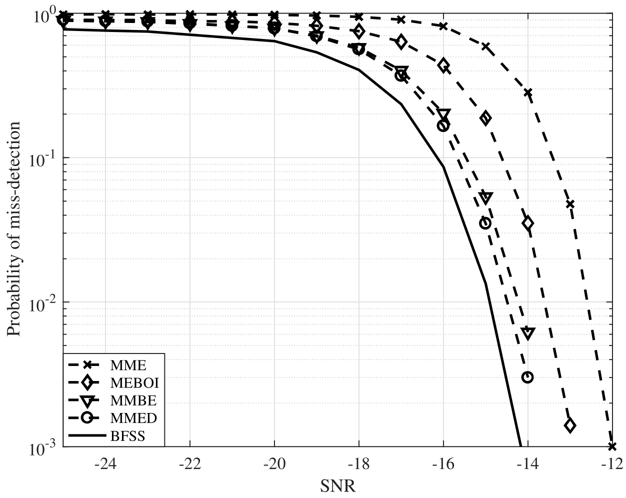

Fig. 2: Probability of miss-detection versus SNR comparing BFSS to other SS algorithms.

Thus, for the same SNR, the detection performance is increased by 10%

c) Simulation results for different values of received antennas M: One of the most important detection features is the number of antenna M. Fig. 3 and 4 illustrate the impact of M value on the performance of the proposed method.

Indeed, the beamforming is spatially more accurate when M increases because there are more directions to scan. In this context, detection performance strongly depends on the number of receiving antennas. In Fig. 3, corresponding to the number of received antenna $M = 3$, the performance decreases drastically comparing to Fig. 2. For an SNR $= -16$ dB, $P_d^{M=3}\{BFSS\} = 0.55$ and $P_d^{M=5}\{BFSS\} = 0.915$. In the case where M increases as depicted in Fig. 4 ($M = 8$), $P_d^{M=8}\{BFSS\} \simeq 1$ for SNR $= -16$ dB. We can also note that the BFSS algorithm performs better than the other methods for all scenarios.

d) Simulation results for different values of observed samples N: The sensing time depends on the number of samples, N. Hence, N represents the signal duration required for SS. On the other hand, it is also the value of N which decides the complexity order. To illustrate the impact of the observed samples, we provide some simulation results in Fig. 6 and Fig. 7 corresponding to $N = 500$ and $N = 4000$ respectively. The 3rd Generation Partnership Project (3GPP) defined the air interface for 5G New Radio (NR), and some specifications are provided for two frequency bands. The first is frequency range 1 (FR1) for frequencies below 6 GHz and frequency range 2 (FR2) for 24 to 54 GHz. In Fig. 5, we provide the allocated sensing time for $N = 500$ and $N = 4000$ for each frequency range of 5G NR. The detection time is certainly important for the SS paradigm but in no case at the expense of reliability. For a fixed probability of detection, for example, $P_d = 0.8$ is reached for a SNR $\simeq -15$ dB in Fig. 6

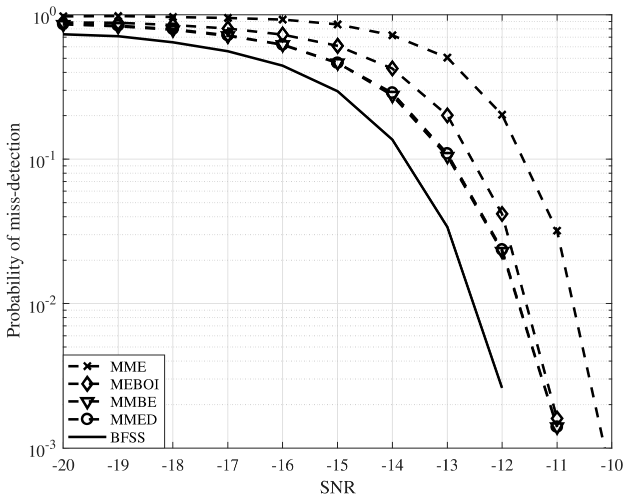

Fig. 3: Probability of miss-detection versus SNR comparing BFSS to other SS algorithms for $M = 3$.

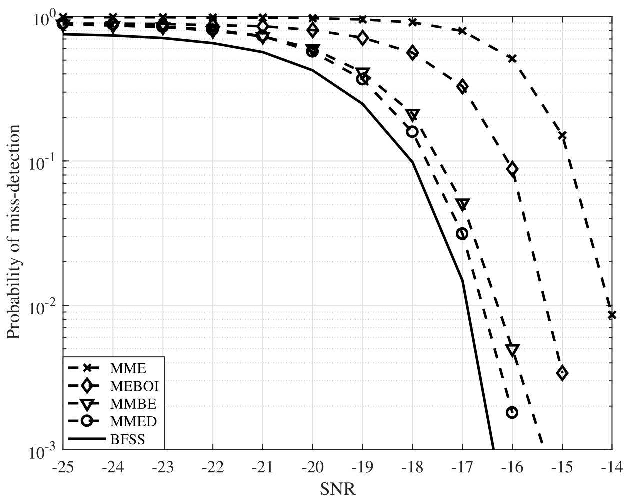

Fig. 4: Probability of miss-detection versus SNR comparing BFSS to other SS algorithms for $M = 8$.

and a SNR $= -20$ dB in Fig. 7, there is a gap of 5 dB for the same performance. The best approach is to provide a good trade-off between complexity and performance for each communication system standard using CR. We can note that the BFSS algorithm outperforms other methods. Indeed, we can see that the provided algorithm gives more than 10% of good detection than the MMED method.

e) Simulation results for different values of AoA (paths) C_p*:* The influence of channel order C_p on the system performance is shown in Fig. 8. The channel order describes the number of AoA. When the frequency selectivity is severe, the performance of the beamforming methods is greatly affected. The channel order impacts all the methods based on the

	Time of detection	
	$N = 500$	$N = 4000$
FR1	5	40
FR2	1.25	10

Fig. 5: Allocated time for SS for FR1 & FR2 in 10^{-6} seconds

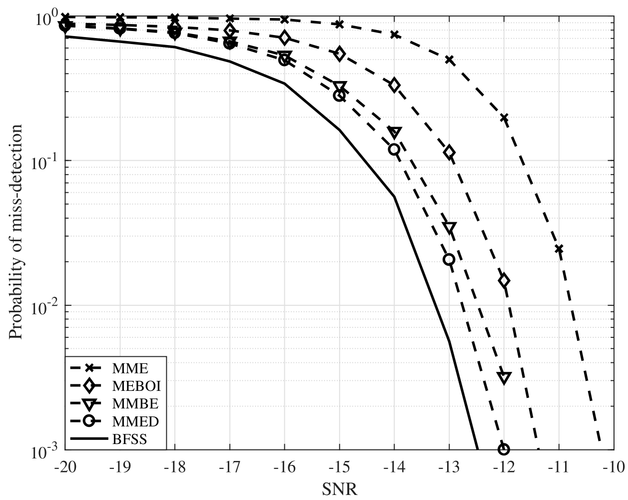

Fig. 6: Probability of miss-detection versus SNR comparing BFSS to other SS algorithms for $N = 500$.

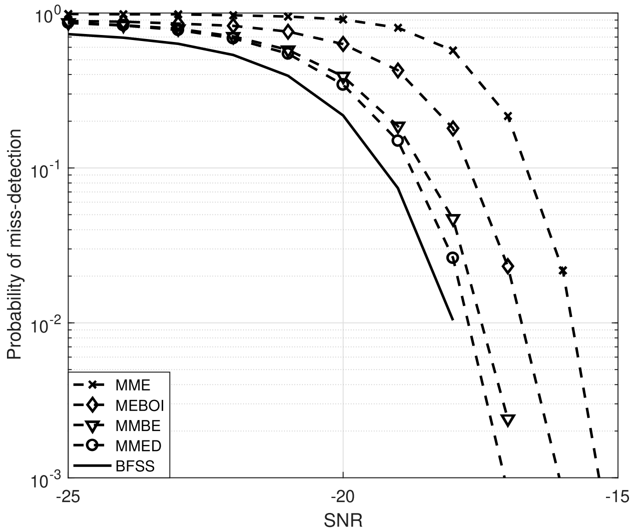

Fig. 7: Probability of miss-detection versus SNR comparing BFSS to other SS algorithms for $N = 4000$.

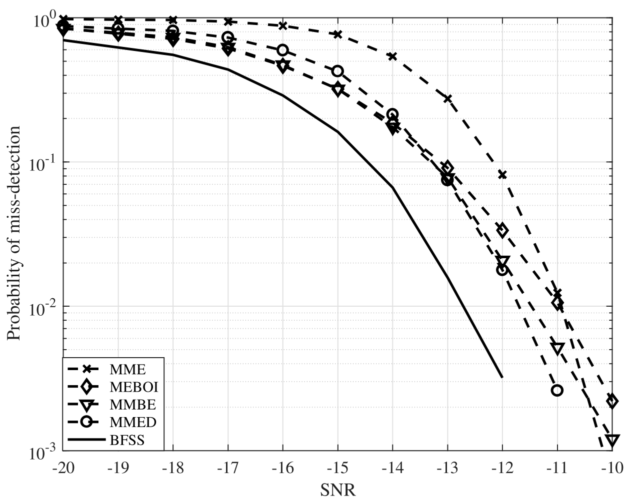

Fig. 8: Probability of miss-detection versus SNR comparing BFSS to other SS algorithms for $C_p = 3$.

beamforming approach, but we can note that the proposed method performs well even for a relatively high number of paths. We can also note that the MME algorithm based on the eigenvalue decomposition of the covariance matrix of the received signal is less impacted than methods based on beamforming. The BFSS algorithm is a good candidate for a severe multipath channel context.

VI. CONCLUSION

This paper proposes a new blind spectrum sensing method in a narrowband context based on an intelligent fusion of spatial filtering. This joint algorithm called Beamforming Fusion assisted Spectrum Sensing (BFSS) aims to exploit results from algorithms based on beamforming. Through simulations, the new blind SS method BFSS outperforms the other beamforming detectors in the literature for the different scenarios. Furthermore, BFSS does not need any knowledge of the noise power, signal, and channel information. In future work, we will focus on the proposed model using a mobile PU under the ray propagation channel and the hidden node problem.

REFERENCES

[1] J. Mitola and J. Maguire, G.Q., "Cognitive radio: making software radios more personal," *IEEE Personal Communications*, vol. 6, pp. 13–18, Aug. 1999.

[2] A. A. Tesfay, E. P. Simon, S. Kharbech, and L. Clavier, "Deep learning-based signal detection for uplink in lora-like networks," in *2021 IEEE 32nd Annual International Symposium on Personal, Indoor and Mobile Radio Communications (PIMRC)*, pp. 617–621, 2021.

[3] B. Mukhopadhyay and T. Samanta, "A smart parking-lot occupancy model in 5g v2v and v2i wireless communication," in *2021 IEEE 32nd Annual International Symposium on Personal, Indoor and Mobile Radio Communications (PIMRC)*, pp. 1552–1557, 2021.

[4] D. Cho and S. Narieda, "Feature detection based computationally efficient spectrum sensing by test statistics sharing among multiple receive antennas," in *2015 IEEE 26th Annual International Symposium on Personal, Indoor, and Mobile Radio Communications (PIMRC)*, pp. 360–264, 2015.

[5] Y. Zeng, Y.-C. Liang, and R. Zhang, "Blindly combined energy detection for spectrum sensing in cognitive radio," *IEEE Signal Processing Letters*, vol. 15, pp. 649–652, 2008.

[6] R. Zhang, T. J. Lim, Y.-C. Liang, and Y. Zeng, "Multi-antenna based spectrum sensing for cognitive radios: A glrt approach," *Communications, IEEE Transactions on*, vol. 58, pp. 84–88, January 2010.

[7] N. Pillay and H. J. Xu, "Eigenvalue-based spectrum 'hole' detection for nakagami-m fading channels with gaussian and impulse noise," *IET Communications*, vol. 6, pp. 2054–2064, Sept 2012.

[8] K. Bouallegue, I. Dayoub, M. Gharbi, and K. Hassan, "Blind spectrum sensing using extreme eigenvalues for cognitive radio networks," *IEEE Communications Letters*, vol. 22, pp. 1386–1389, July 2018.

[9] T. Baykas, L. Goratti, T. Rasheed, and S. Kato, "On the spectrum efficiency of mesh and star topology wide area wireless sensor networks," in *2014 IEEE 25th Annual International Symposium on Personal, Indoor, and Mobile Radio Communication (PIMRC)*, pp. 1819–1823, 2014.

[10] K. Bouallegue, I. Dayoub, and M. Gharbi, "On low-complexity spectrum sensing: Analytical approach based spatial scanning," in *2017 IEEE Wireless Communications and Networking Conference (WCNC)*, pp. 1–6, March 2017.

[11] K. Bouallegue, I. Dayoub, M. Gharbi, and K. Hassan, "A cost-effective approach for spectrum sensing using beamforming," *Physical Communication*, vol. 22, no. Supplement C, pp. 1 – 8, 2017.

[12] K. Bouallegue, I. Dayoub, and M. Gharbi, "Spectrum sensing for wireless communications using energy ratio and beamforming," in *2017 IEEE International Conference on Communications (ICC)*, pp. 1–6, May 2017.

[13] O. P. Awe, A. Deligiannis, and S. Lambotharan, "Spatio-temporal spectrum sensing in cognitive radio networks using beamformer-aided svm algorithms," *IEEE Access*, vol. 6, pp. 25377–25388, 2018.

[14] N. A. Khalek and W. Hamouda, "Learning-based cooperative spectrum sensing in hybrid underlay-interweave secondary networks," in *GLOBECOM 2020 - 2020 IEEE Global Communications Conference*, pp. 1–6, 2020.

[15] N. A. Khalek and W. Hamouda, "Unsupervised two-stage learning framework for cooperative spectrum sensing," in *ICC 2021 - IEEE International Conference on Communications*, pp. 1–6, 2021.

[16] K. Bouallegue, I. Dayoub, and M. Gharbi, "Blind spectrum sensing based spatial scanning and maximum energy ratio," in *Proceedings in progress 24rd International Conference on Software, Telecommunications and Computer Networks (SoftCOM), 2016*, Sept 2016.

[17] S. M. Kay, *Fundamentals of Statistical Signal Processing, Volume 2: Detection Theory*. Englewood Cliffs, NJ: Prentice Hall, 1998.

[18] Y. Zhao, J. Huang, W. Wang, and R. Zaman, "Detection of primary user's signal in cognitive radio networks: Angle of arrival based approach," in *2014 IEEE Global Communications Conference*, pp. 3062–3067, Dec 2014.

[19] C. Balanis, *Antenna Theory: Analysis and Design*, ch. 6, pp. 284–303. Wiley-Interscience; 3rd edition, 2005.

[20] K. Bouallegue, I. Dayoub, M. Gharbi, and K. Hassan, "A cost-effective approach for spectrum sensing using beamforming," *Physical Communication*, pp. –, 2016.

[21] Y. Zeng and Y.-C. Liang, "Eigenvalue-based spectrum sensing algorithms for cognitive radio," *IEEE Transactions on Communications*, vol. 57, pp. 1784–1793, Jun. 2009.